journal

J. Am. Ceram. Soc., 93 [12] 4129–4134 (2010)
DOI: 10.1111/j.1551-2916.2010.04002.x

Enhanced Photochemical Reactivity at the Ferroelectric Phase Transition in $Ba_{1-x}Sr_xTiO_3$

Abhilasha Bhardwaj, Nina V. Burbure, and Gregory S. Rohrer*,†

Department of Materials Science and Engineering, Carnegie Mellon University, Pittsburgh, Pennsylvania 15213-3890

Optical absorption and reflectance spectroscopy have been used to monitor the photochemical reactivity of $Ba_{1-x}Sr_xTiO_3$ solid solutions with aqueous solutions containing methylene blue. Atomic force microscopy indicates that methylene blue is reduced on the surfaces of domains that have a positive surface polarization. The results indicated that $SrTiO_3$ and $BaTiO_3$ have similar reactivities. As the second component is added to either of the pure materials, the reactivity decreases. However, there is a sharp maximum in reactivity at the tetragonal-to-cubic phase boundary. This is attributed to the anomalously high dielectric constant at this composition that increases the width of the space charge region and charge carrier separation in the near surface region.

I. Introduction

PARTICULATE semiconductors can be used as relatively inexpensive catalysts for photochemical reactions such as water splitting.[1] However, the recombination of photogenerated electron-hole pairs within the particle, and the recombination reaction products on the surface of the particle are two factors that reduce efficiency. Ferroelectrics are of interest as photocatalysts because they have internal dipolar fields that may separate both the electron-hole pairs and the products of the redox reactions. If this separation occurs, it may reduce recombination losses. Both single-phase ferroelectrics and composites involving ferroelectrics have been investigated and some promising results have been reported.[2–9] Atomic force microscopy (AFM) studies have also documented the fact that the products of the redox reactions on single phase and composite materials occur on spatially distinct locations.[10–13]

The mechanism for the charge separation is thought to be related to the effect of polarization on the near surface space charge region. For domains in which the positive end of the polarization vector points toward the surface (positive domains), it is assumed that the positive charge draws compensating electrons toward the surface and either reduces the band bending that would occur on an unpolarized surface or even bends the bands downward creating an accumulation layer. The opposite occurs on negative domains, where the polarization repels electrons from the surface and bends the bands further upward with respect to the neutral surface, creating a depletion layer. While this model is consistent with most observations,[10–16] the effect of the strength of polarization on photochemical reactions has not been studied in detail.

The purpose of this paper is to compare the relative reactivities of $Ba_{1-x}Sr_xTiO_3$ samples with a range of polarizations. At the outset, it should be noted that it is not possible to change the strength of the polarization without simultaneously altering some other parameter (composition or temperature) that also has the potential to influence the reactivity. One promising route is to vary the composition of a ternary material to alter the polarization without substantially changing the structure. For example, $SrTiO_3$ and $BaTiO_3$ are mutually soluble and can be reacted to form $Ba_{1-x}Sr_xTiO_3$, where $0 \leq x \leq 1$.[17] $BaTiO_3$ is ferroelectric at room temperature and has a remnant polarization of 26 $\mu C/cm^2$.[18] As x increases, the polarization is reduced until it disappears completely at $x \sim 0.3$.[19] The band gaps of $SrTiO_3$ and $BaTiO_3$ are also quite similar. If one considers various measurements of band gaps in the bulk materials, it is apparent that both are approximately 3.2 eV and that the band gap of $BaTiO_3$ is about 100 mV higher than $SrTiO_3$.[20–25] The positions of the conduction band edges are also similar, with the $BaTiO_3$ conduction band edge being 50 mV higher than that of $SrTiO_3$.[26]

Ohara *et al.*[27] reported the photochemical reduction of silver on a thin film that was compositionally graded in one spatial dimension from pure $SrTiO_3$ to pure $BaTiO_3$. The amounts of silver were related to changes in the band gap and they found that the transition from the ferroelectric to nonferroelectric phase occurred over a wide composition range. The results indicate that in the composition domain where the samples are ferroelectric, less silver is reduced than by the nonferroelectric samples. A more recent report by Tiwari *et al.*[28] compares the ability of lead zirconate titanate with two different Zr/Ti ratios to photochemically reduce silver. The differences in the reaction of the two compositions was attributed to differences not only in the polarization, but also in the band gap and carrier concentration. In both of the reports discussed above, the materials had fine grain sizes. When the particle size approaches twice the width of the space charge region, the band bending is reduced.[29] For the cases of interest here, space charges widths for depletion layers are probably in the range of 10–30 nm. Therefore, the effects of ferroelectric polarization or changes in polarization may not be as apparent in nanostructured materials with grain sizes on the order of 50 nm.

In the present paper, we report on the photochemical reaction of $Ba_{1-x}Sr_xTiO_3$, in the composition range of $0 \leq x \leq 1$, with aqueous methylene blue solutions. Methylene blue is a common indicator for reduction and oxidation processes because it changes color when it gains or loses an electron.[30] Also, its reduction potential (0.01 V on the NHE scale at pH 7) is very near that of hydrogen.[31] The results here show that when solid pellets of $Ba_{1-x}Sr_xTiO_3$ were illuminated with UV light in aqueous methylene blue solution, the solution becomes less blue while the surface of the pellet comes more blue. The accumulation of methylene blue on the sample surface was studied with diffuse reflectance spectroscopy and AFM. The decoloration of the solution was evaluated with optical absorption spectroscopy. The results show that there is a maximum in the reactivity at the composition of near the phase boundary between the ferroelectric and nonferroelectric phase. This is most likely related to the changes in the dielectric constant as a function of composition, which affect the width of the space charge region.

A. Srivastava—contributing editor

Manuscript No. 27676. Received March 15, 2010; approved June 22, 2010.
The work was supported by National Science foundation grants DMR 0412886 and DMR 0804770.
*Member, The American Ceramic Society.
†Author to whom correspondence should be addressed. e-mail: gr20@andrew.cmu.edu

II. Experimental Methods

Cylindrical, polycrystalline pellets of $Ba_{1-x}Sr_xTiO_3$ in the composition range of $0 \leq x \leq 1$ were synthesized by conventional powder processing techniques from $BaTiO_3$ (99.7% Alpha Aesar, Ward Hill, MA) and $SrTiO_3$ (99.9% Alpha Aesar). Appropriate amounts of the two starting materials were mixed and pellets were formed by pressing the powders (with a few drops of ethanol as a binder) in a 1 cm diameter cylindrical die with a uniaxial load of 230 MPa. The pellets were then degassed at 900°C in air for 10 h and then reacted in air at 1250°C for 12 h. After reaction, the pellets were pulverized; powder X-ray diffraction was used to verify that a single-phase solution was obtained. New pellets were made from the prereacted powders, which were sintered in air at 1250°C for 6 h. The pure materials with $x = 0$ and 1 were processed in the same way, except that the pure $SrTiO_3$ was sintered at 1300°C.

An important consideration for the diffuse reflectance measurements was that the samples all have the same color and appearance. The sintering conditions for the samples were selected so that they would remain white and colorless, but still have enough mechanical stability for handling. As a result, the samples are relatively porous. They were comprised of sintered particles with a range of sizes, from about 500 nm to 2 μm in agglomerates, with occasional crystals with sizes greater than 5 μm. Characteristic SEM images are shown in Figs. 1(a)–(c). Because the samples were sintered solids, the reaction was confined to the illuminated surface. Differences in surface roughness can change the effective surface area, but the micrographs in Figs. 1(a)–(c) indicate that roughnesses are comparable. Therefore, it was assumed that the surface area was the same for all of the samples.

One sample with a higher concentration of donors was created by doping with 0.5 mol% yttria. At this composition, it is assumed that each Y^{3+} substitutes on a Ba^{2+} site and is compensated by a donor electron.[32] In Kroger–vink notation, this dissolution reaction can be expressed in the following way:

$$Y_2O_3 + 2TiO_2 = 2Y^{\bullet}_{Ba} + 2Ti_{Ti} + 6O_O + 1/2O_2 + 2e' \quad (1)$$

A sample with 0.5 mol% yttria was created by combining appropriate amounts of 99.999% pure Y_2O_3 powder (Acros Organics, Morris Plains, NJ) with $BaTiO_3$ and ball milling. A pellet was formed as described previously, reacted at 1000°C for 90 min and then reground. A new pellet was formed, degassed at 900°C for 10 h, sintered at 1230°C for 10 h. For the AFM experiments, one dense $BaTiO_3$ sample was created using the same procedure, but no yttria was added and the final sintering step was 1360°C for 3 h. Methylene blue dye was obtained from Fisher Scientific in powder form. This dye powder was dissolved in deionized water. A concentrated dye solution ($4 \times 10^{-5} M$) was made in large quantity batches (4 L per batch). This solution was diluted to the desired concentrations for the experiments.

All reactions were carried out in a 250 mL reactor with a 1 in. diameter, flat quartz window. Pellets were suspended in the reactor so that one face was parallel to and near the window. Two hundred milliliters of methylene blue solution ($5 \times 10^{-6} M$) was added to the reactor and this was magnetically stirred throughout the course of the experiment. After the initial 10 min of stirring, illumination was supplied by a 300 W mercury lamp. The qualitative observation of these experiments was that with increasing exposure times, the portions of the pellet surface reached by the light became more and more blue while the solution became less and less blue. The surfaces of the pellet not directly illuminated remained colorless. The process was investigated in more detail using AFM and optical spectroscopy.

Noncontact topographic AFM images and surface potential microscopy (SPM) images were obtained using a Veeco Digital

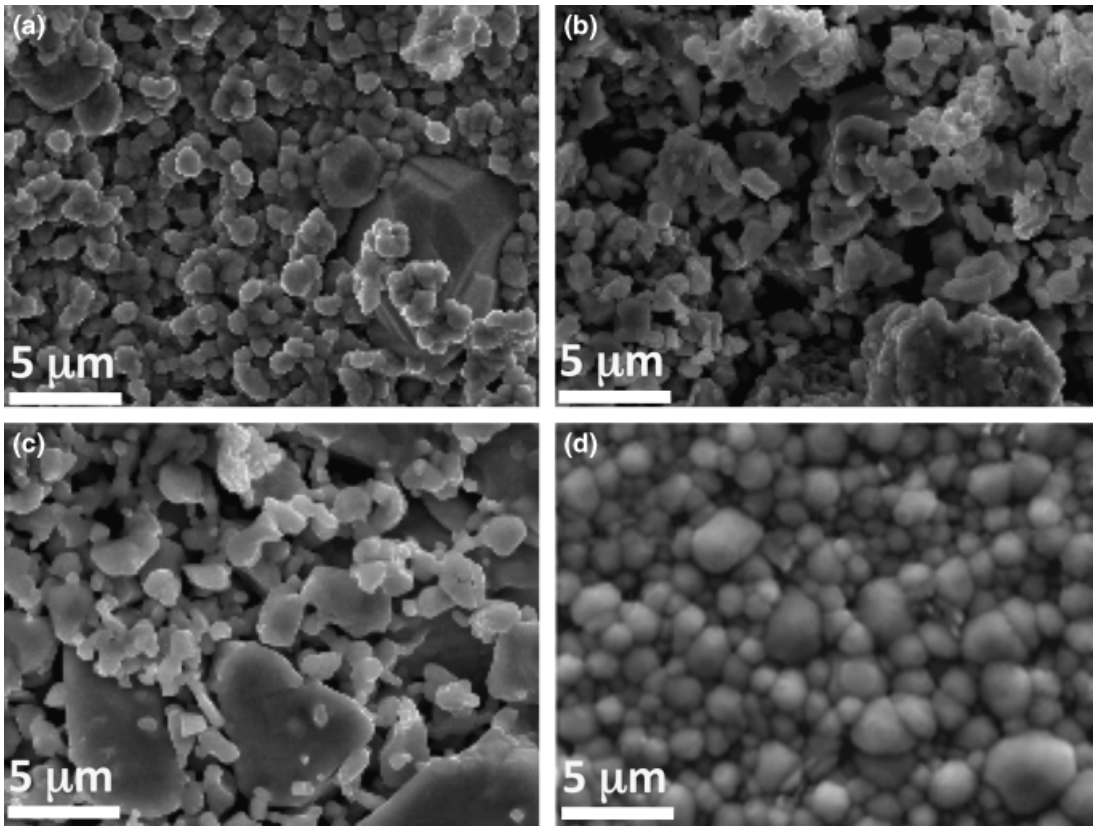

Fig. 1. Secondary electron SEM images of the surfaces of (a) $BaTiO_3$, (b) $Sr_{0.8}Ba_{0.2}TiO_3$, (c) $SrTiO_3$, and (d) 0.5 mol% Y_2O_3-doped $BaTiO_3$ samples used for the spectroscopy experiments.

Instruments Dimension 3100 AFM (Plainview, NY). The $BaTiO_3$ was suspended in $1 \times 10^{-5} M$ methylene blue solution and illuminated for 100 min, and then imaged. The dye was then removed by sonication in acetone for 20–30 min, and topographic and SPM images of the same location were recorded.

The changes in the color of the dye solution and the solid surface were studied by optical absorption and reflectance, respectively. All optical absorption and reflectance measurements were made using an Ocean Optics USB 2000 UV–VIS spectrometer (Model AIS MINI DT B) (Dunedin, FL). In the case of the absorption measurements, 5 mL solution samples were removed from the reactor at 40-min intervals over the course of 200 min, and absorption spectra were measured. The spectra also showed a strong absorption band centered at about 667 nm that is characteristic of methylene blue absorption.[33] To reduce noise, the absorbance was determined by averaging the values from 650 to 675 nm. For the reflectance experiments, the solid sample was removed after 40 min and four reflectance spectrum were obtained. The spectra showed a broad minimum at 656 nm so the values of the reflectance at this point were averaged and taken as the reflectance of each sample. Samples of $Ba_{1-x}Sr_xTiO_3$ with 12 different values of x were studied by both methods.

A number of control experiments were also conducted to test the validity of the methods and assess uncertainty. First, it was verified that the absorption of methylene blue dye solutions as a function of concentration obeys Beer's law between 5×10^{-6} and $1 \times 10^{-5} M$. Second, experiments without UV illumination were conducted. For example, the absorbance of a methylene blue solution exposed only to room light was monitored for 200 min. An identical solution, containing a $SrTiO_3$ sample, was also monitored. In both cases, there was no measureable change in the color of the solution. There were, however, small fluctuations in the measured average absorbance of 1.2%. Therefore, this is used as a measure of uncertainty for all absorbance measurements. Note also that in all experiments with UV illumination, the portion of the pellets not directly illuminated remained colorless, showing that UV light is necessary for the color change. Third, an experiment was conducted using an Al_2O_3 sample in place of the $Ba_{1-x}Sr_xTiO_3$. Because of aluminum oxide's large band gap, the UV lamp used in this study is not capable of generating electron-hole pairs. During the course of this experiment, the Al_2O_3 remained colorless. The methylene blue solution did decrease slightly in absorbance, but by less than 20% of the change in a typical experiment with $Ba_{1-x}Sr_xTiO_3$. This background decoloration process is assumed to occur homogeneously in all of the experiments.

Because of interactions between the methylene blue solution and the $Ba_{1-x}Sr_xTiO_3$ samples with different compositions, there are small changes in the pH of the solution and this might potentially affect the decoloration. The pH of the initial solution is 6.5 and it becomes slightly acidic (by 0.05–0.3 pH units) after the samples are added. To test the potential effect of pH on reactivity, one sample was also analyzed in a methylene blue solution made slightly acidic (pH 5.6) by the addition of H_2SO_4 and another made slightly basic (pH 7.2) by the addition of NaOH. The rate of decoloration of the solutions with pH 5.6 and 7.2 varied by less than 20% from the solution at pH 6.5. Because these excursions in pH did not dramatically affect the reactivity, we assume the smaller changes in pH that occur in the experiment are not influential.

When the variation in absorbance with composition is considered, there are unavoidable variations in the initial absorbance values that arise from small variations in the exact concentration of the solution and from interactions between the sample and solution when they are combined. All of the average absorption values were corrected so that they had the same initial value. The average correction was about 1% of the absorbance value. This correction does not change any of the trends with composition that are discussed in the next section.

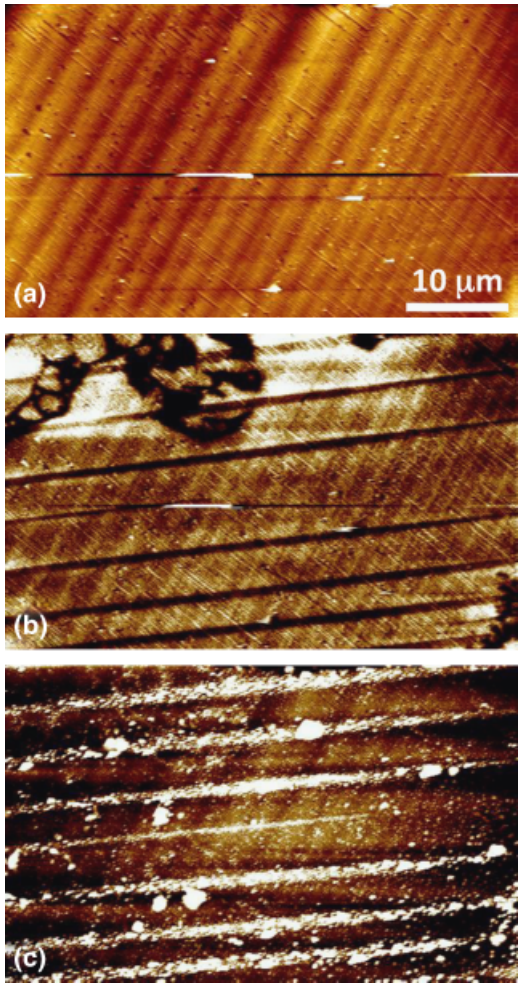

Fig. 2. (a) A topographic atomic force microscopy (AFM) image of the $BaTiO_3$ surface. Black-to-white contrast is 65 nm. The horizontal line in the center of the image is an artifact from an instability during the scan. (b) A surface potential image acquired simultaneously with the image in (a), revealing the domain structure. The black-to-white contrast is 50 mV. (c) A topographic AFM image of the same location after reaction with the dye. Here, the black-to-white contrast is 100 nm.

III. Results

A topographic AFM image of $BaTiO_3$ before a reaction is shown in Fig. 2(a). The contrast is the result of small facets or surface steps. The surface potential image in Fig. 2(b), recorded at the same time as Fig. 2(b), shows straight lines of black contrast that correspond to 90° domains. It was shown by Kalinin *et al.*[34] that regions with a negative potential (dark contrast) correspond to positive domains (those with a component of the polarization directed away from the surface) while regions of positive potential are negative domains. The apparent reversal of the potential occurs because it is actually the screening charge of the surface adsorbate layer that is sensed in the potential image, not the domain.[34] A topographic AFM image of the same location on the surface after the reaction with the methylene blue is shown in Fig. 2(c). White contrast, indicating a topographically higher area, has clearly accumulated on the same locations as the positive domains in Fig. 2(b). We assume that this accumulated material is a product of the reaction between the sample and methylene blue solution and is responsible for the appearance of color on the sample. Furthermore, because the product accumulates on the positive domains, we infer that this is the product of a reduction reaction.[10,11]

The composition dependence of the reflectance of $Ba_{1-x}Sr_xTiO_3$ samples at 657 nm is shown in Fig. 3. As the sample become bluer, it reflects less light. Note that the vertical scale has been inverted to emphasize the fact that reduced reflectance is

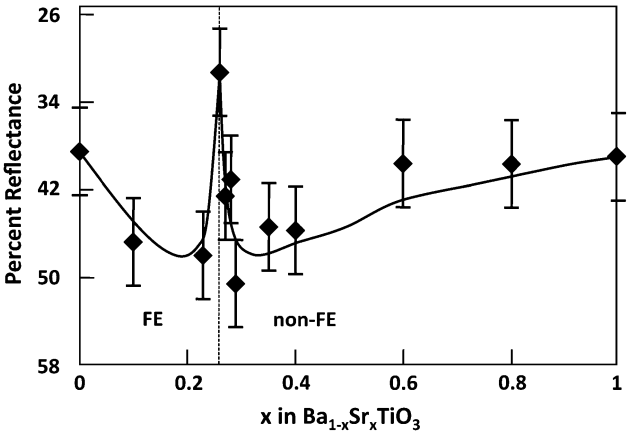

Fig. 3. The composition dependence of the reflectance of $Ba_{1-x}Sr_xTiO_3$. Note that the reflectance scale is deliberately inverted so that vertical increases correlate to increasing reactivity. The solid line is drawn as a guide to the eye. The vertical dashed line separates ferroelectric (FE) from nonferroelectric (non-FE) compositions.

associated with a greater extent of reaction. The experiment was conducted twice with the same samples. The points in the figure indicates the average of the two results and the error bar indicates the standard deviation of the measured values from the average. The overall trend in the data is that as x increases from 0 or decreases from 1, the relative reactivity decreases. However, there is also a local maximum in reactivity at $x = 0.26$. This is the composition at which the Curie temperature of $Ba_{1-x}Sr_xTiO_3$ is very near room temperature. Therefore, this composition is on the boundary between the ferroelectric ($x < 0.26$) and nonferroelectric phases ($x > 0.26$).

The absorbance spectra of the methylene blue dye solution was recorded every 40 min during one experiment. The peak absorbance as a function of time for four representative specimens shown in Fig. 4. The decay in absorbance is linear with time, indicating a zero-order reaction. This results from the approximately planar nature of the interface to which the reaction is confined. As long as the surface is saturated with methylene blue, the reaction rate will be independent of the concentration in solution and depend only on the intensity of the light and the illuminated area. Figure 5 shows the average absorbance after 200 min of exposure as a function of composition. Note again the scale is inverted so that reduced absorbance, which corresponds to higher reactivity, is shown as an increase. These results show the same general trend as the reflectance. As x increases from 0 or decreases from 1, the relative reactivity decreases, and there is a local maximum in reactivity near the composition where $Ba_{1-x}Sr_xTiO_3$ changes from ferroelectric to nonferroelectric.

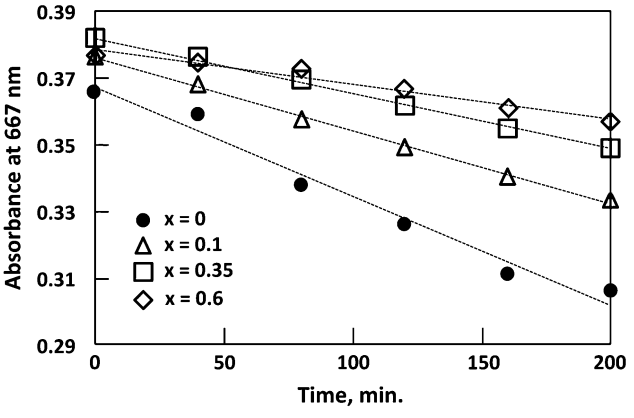

Fig. 4. Time dependence of the peak absorbance for four samples: $x = 0$, $x = 0.1$, $x = 0.35$, and $x = 0.6$.

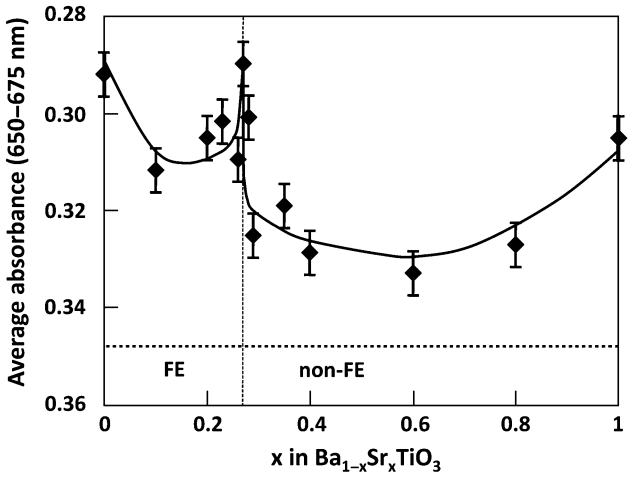

Fig. 5. Absorption of the $5 \times 10^{-6} M$ methylene blue solution after 200 min exposure in the presence of $Ba_{1-x}Sr_xTiO_3$, versus composition, x. Note that the absorbance scale is deliberately inverted so that vertical increases correlate to increasing reactivity. The vertical dashed line separates ferroelectric (FE) from nonferroelectric (non-FE) compositions and the horizontal dashed line marks the absorbance at 0 min. The error bars are an estimate of the uncertainty, based on repeated experiments using samples of the same composition.

To examine the influence of donor concentration on reactivity, the rate of decoloration of the methylene blue solution for pure $BaTiO_3$ was compared with the decoloration rate for yttria-doped $BaTiO_3$. The change in absorbance with time is shown in Fig. 6. The data indicate that the undoped specimen degrades the dye at a faster rate than the doped specimen.

IV. Discussion

It is assumed that, during these reactions, both the reduced (blue) and oxidized (colorless) forms of the dye are present in solution. As the reaction proceeds, the surface of the $Ba_{1-x}Sr_xTiO_3$ becomes more and more blue. The most likely cause of this is that the reduced form of the dye is deposited on the surface. The AFM images show that material collects on the surfaces of positive domains. These are the same domains that have been observed to reduce Ag^+ to Ag in other work.[10,11] Therefore, it seems likely that the material collecting on these domains is the reduced form of the dye. Note that the heights of these deposits are many 10 s of nanometers and this change in topography can not be explained by simple monolayer molecular absorption.

There is an oxidation reaction happening in parallel to the reduction and this is the source of the decoloration of the

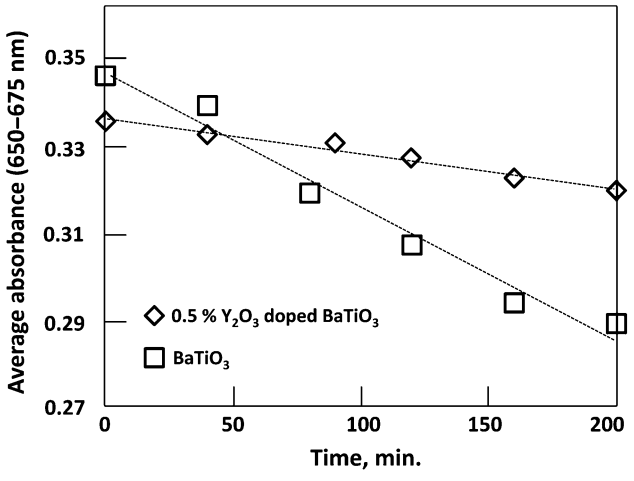

Fig. 6. Absorption of methylene blue solution versus time for $BaTiO_3$ and 0.5 mol% Y_2O_3-doped $BaTiO_3$.

solution. One mechanism can be that the dye molecules in the reduced state are directly oxidized by the absorption of a hole and they loose their color. The second mechanism is that the oxidation reaction produces hydroxyl radicals that later oxidize the methylene blue molecule. Beyond the initial removal of an electron that changes the molecule's absorption characteristics, additional hydroxyl radicals may continue to attack and eventually mineralize the molecule. In all likelihood, both processes contribute to the decoloration of the solution.[30]

Considering the discussion above, we can infer that the reflectance measurements monitor the reduction process and the absorbance measurements monitor the oxidation process. The fact that the composition dependence of the reduction (see Fig. 3) and the oxidation (see Fig. 5) are similar suggests that the overall reaction has the same composition dependence. Of course, charge neutrality demands that reduction and oxidation occur at the same rate. It should also be noted that in a separate set of experiments, the composition dependence of the photochemical reduction of silver by $Ba_{1-x}Sr_xTiO_3$ was consistent with the current findings.[35]

The composition dependence of the reactivity is potentially influenced by a number of factors. For example, the band gaps of the samples are not identical. As mentioned in the introduction, a review of the band gap measurements reveals that the band gap of $SrTiO_3$ is probably about 100 mV smaller than $BaTiO_3$, implying that $SrTiO_3$ will absorb more light than $BaTiO_3$ and potentially be more reactive. Assuming a smooth transition for the intermediate compositions, we would expect an increase in reactivity as the composition changes from pure $BaTiO_3$ to pure $SrTiO_3$. This is not consistent with the observations, and therefore we conclude that the change is band gap is not a dominant factor in determining the composition dependence of the reactivity. However, it should also be mentioned that the composition dependence of the photochemical reduction of silver in nanostructured $Ba_{1-x}Sr_xTiO_3$ thin films, which do not exhibit band bending, was explained by changes in the band gap.[27] For that case, both the composition dependence of the reactivity and the band gaps differed substantially from the bulk material described here.[27]

Polarization within the domains changes dramatically as a function of composition and this also has the potential to affect the reactivity. Room temperature polarization data reported by Ianculescu *et al.*[19] indicates that the polarization decreases by about 1/3, from 26 to 17.5 $\mu C/cm^2$, as the Sr content increases from $x = 0$ to $x = 0.3$. There is then a precipitous decrease to zero at the tetragonal to cubic transition and the polarization then remains zero for all compositions richer in Sr. If it is assumed that polarization enhances reactivity by separating electron hole pairs and reducing recombination, then one would expect a continuous decrease in reactivity as Sr is added to $BaTiO_3$, and a sharp drop at the transition. While the initial decrease in reactivity as Sr is added is consistent with this idea, the local maximum just before the transition cannot be explained by the composition dependence of the polarization.

Another factor that might affect the reactivity is solid solution scattering of the charge carriers. Sr added to $BaTiO_3$, or Ba added to $SrTiO_3$, create nonperiodic features in the crystal structure that can scatter electrons and holes. This scattering increases recombination and, therefore, is expected to decrease reactivity. This is consistent with the composition dependence of the reactivity shown in Figs. 3 and 5. While the initial decrease in reactivity as the solid solution becomes more concentrated is consistent with alloy scattering, it does not explain the sharp peak in reactivity at the transition composition.

One physical parameter of these solid solutions that varies discontinuously with composition is the dielectric constant. Nowotny and Rekas[36] report that the dielectric constants of $SrTiO_3$ and $BaTiO_3$ are approximately 220 and 1250, respectively. Furthermore, for all compositions of $Ba_{1-x}Sr_xTiO_3$, there is a sharp maximum in the dielectric constant at the cubic to tetragonal transition temperature. For samples with a composition of $x = 0.3$, the dielectric constant reaches as maximum of 12 500 near room temperature and drops precipitously above the transition temperature.[36] Therefore, in the experiments described here, we expect the dielectric constant to reach this maximum at the composition where the sample transforms from tetragonal to cubic.

The increase in the dielectric constant can influence the photochemical reactivity through its effect on the width of the space charge region created by band bending at the solid–liquid interface. Because the sloping bands help to separate the photogenerated electrons and holes, it is mostly the carriers generated in the space charge region that participate in the surface reactions; those generated further within the sample, where the bands are flat, are not effectively transported to the surface. Whether the bands are bent in depletion or in accumulation, the width of the space charge region is proportional to the Debye length, L_D:

$$L_D = \left(\frac{\varepsilon_0 \varepsilon_r kT}{e^2 N_D}\right)^{1/2} \tag{2}$$

where ε_0 is the permittivity of free space, ε_r is the dielectric constant, and N_D is the donor density. While we do not know the donor density of our samples, based on previous measurements for $BaTiO_3$, we can estimate it to be $3 \times 10^{19}/cm^3$.[37] Thus, for $BaTiO_3$ and $SrTiO_3$ we can estimate the Debye lengths to 7.7 and 3.2 nm, respectively. If the dielectric constant increases by a factor of 10 at the transition, the Debye length will increase by a factor of 3. As the volume of the space charge region increases, more of the photogenerated electrons and holes can participate in the reaction. This feature can explain the enhanced reactivity at the transition, and the abrupt decrease in reactivity after the reaction.

The explanation given above can only apply in the case where the light is absorbed throughout the space charge region, regardless of its width. The absorption coefficients of $BaTiO_3$ and $SrTiO_3$ have been measured near the band edge and are reported to be in the range of 1×10^4 cm^{-1}, depending on the source.[21–25] Therefore, the absorption depth is expected to be about 350 nm. The space charge width in depletion, L_d, depends on the Debye length and the surface potential, V_s

$$L_d = \left(\frac{2eV_s}{kT}\right)^{1/2} L_D \tag{3}$$

Assuming $V_s = 0.5$ V at room temperature, the maximum space charge width is < 50 nm. The space charge width for the case of accumulation is even smaller. Because electron-hole pairs should be generated at depths that exceed the maximum space charge width, a widening of the space charge will increase the number of electron hole pairs that are separated.

For $SrTiO_3$ and $BaTiO_3$ in aqueous solution, the bands are thought to be bent slightly upwards at the solid–liquid interface. For the ferroelectric sample, the band bending it expected to vary as a function of position on the surface. In domains that are positively polarized on the surface, the bands are bent downward from their unpolarized level and if negatively polarized, the bands are bent further upward. Past observations of reactions on ferroelectrics are consistent with the idea that electrons are promoted to the surfaces of positive domains with downward band banding and holes are promoted to negatively polarized surfaces with upward band bending.[10–16]. Regardless of the direction of the band banding, an increase in the Debye length increases the width of the space charge region.

By the same rationale, a decrease in the Debye length should reduce the photochemical reactivity. According to Eq. (2), the Debye length can be decreased by increasing the donor concentration. The Y-doped specimen, which had a donor concentration of $9 \times 10^{19}/cm^3$, should reduce the Debye length by approximately one half, assuming complete ionization. This is consistent with the observation that increasing the donor concentration decreases the rate at which methylene blue is

degraded (see Fig. 6). It should be noted that Y-doping is also expected to increase the rate of ionized impurity scattering and this may also contribute the reduced reactivity of the doped sample.

V. Conclusions

$BaTiO_3$, $SrTiO_3$, and $Ba_{0.73}Sr_{0.26}TiO_3$ (which is at the composition were the phase transforms from tetragonal to cubic) degrade methylene blue dye similar rates. For intermediate compositions, the composition dependence of the dielectric constant, solid solution scattering, and remnant polarization influence the reactivity. The dominant factor is the anomalously high dielectric constant at the tetragonal to cubic transformation composition that increases the width of the space charge region and, with it, the rate at which methylene blue is degraded.

Acknowledgments

The authors thank Pranay Choudhary in obtaining SEM images.

References

[1]F. E. Osterloh, "Inorganic Materials as Catalysts for Photochemical Splitting of Water," *Chem. Mater.*, **20** [1] 35–54 (2008).

[2]H. van Damme and W. K. Hall, "Photocatalytic Properties of Perovskites for H_2 and CO Oxidation—Influence of Ferroelectric Properties," *J. Catal.*, **69** [2] 371–83 (1981).

[3]Y. Inoue, I. Yoshioka, and K. Sato, "Polarization Effects Upon Adsorptive and Catalytic Properties. 1. Carbon Monoxide Oxidation over Palladium Deposited on Lithium Niobate ($LiNbO_3$) Ferroelectrics," *J. Phys. Chem.*, **88** [6] 1148–51 (1984).

[4]Y. Inoue, K. Sato, and S. Suzuki, "Polarization Effects Upon Adsorptive and Catalytic Properties. 2. Surface Electrical Conductivity of Nickel(II) Oxide Deposited on Lithium Niobate ($LiNbO_3$) and its Changes Upon Gas Adsorption," *J. Phys. Chem.*, **89** [13] 2827–31 (1985).

[5]Y. Inoue, M. Okamura, and K. Sato, "A Thin-Film Semiconducting Titanium Dioxide Combined with Ferroelectrics for Photoassisted Water Decomposition," *J. Phys. Chem.*, **89** [24] 5184–7 (1985).

[6]Y. Inoue, K. Sato, K. Sato, and H. Miyama, "A Device Type Photocatalyst Using Oppositely Polarized Ferroelectric Substrates," *Chem. Phys. Lett.*, **129** [1] 79–81 (1986).

[7]Y. Inoue, K. Sato, K. Sato, and H. Miyama, "Photoassisted Water Decomposition by Ferroelectric Lead Zirconate Titanate Ceramics with Anomalous Photovoltaic Effects," *J. Phys. Chem.*, **90** [13] 2809–10 (1986).

[8]Y. Inoue, O. Hayashi, and K. Sato, "Photocatalytic Activities of Potassium-Doped Lead Niobates and the Effect of Poling," *J. Chem. Soc., Faraday Trans.*, **86** [12] 2277–82 (1990).

[9]R. R. Yeredla and H. Xu, "Incorporating Strong Polarity Minerals of Tourmaline with Semiconductor Titania to Improve the Photosplitting of Water," *J. Phys. Chem. C*, **112** [2] 532–9 (2008).

[10]J. L. Giocondi and G. S. Rohrer, "Spatially Selective Photochemical Reduction of Silver on the Surface of Ferroelectric Barium Titanate," *Chem. Mater.*, **13** [2] 241–2 (2001).

[11]J. L. Giocondi and G. S. Rohrer, "Spatial Separation of Photochemical Oxidation and Reduction Reactions on the Surface of Ferroelectric Barium Titanate," *J. Phys. Chem. B*, **105** [35] 8275–7 (2001).

[12]N. V. Burbure, P. A. Salvador, and G. S. Rohrer, "Influence of Dipolar Fields on the Photochemical Reactivity of Thin Titania Films on $BaTiO_3$ Substrates," *J. Am. Ceram. Soc.*, **89** [9] 2943–5 (2006).

[13]J. L. Giocondi and G. S. Rohrer, "The Influence of the Dipolar Field Effect on the Photochemical Reactivity of $Sr_2Nb_2O_7$ and $BaTiO_3$ Microcrystals," *Top. Catal.*, **49** [1–2] 18–23 (2008).

[14]S. V. Kalinin, D. A. Bonnell, T. Alvarez, X. Lei, Z. Hu, J. H. Ferris, Q. Zhang, and S. Dunn, "Atomic Polarization and Local Reactivity on Ferroelectric Surfaces: A New Route toward Complex Nanostructures," *Nano Lett.*, **2** [6] 589–93 (2002).

[15]J. N. Hanson, B. J. Rodriguez, R. J. Nemanich, and A. Gruverman, "Fabrication of Metallic Nanowires on a Ferroelectric Template Via Photochemical Reaction," *Nanotechnology*, **17** [19] 4946–9 (2006).

[16]S. Dunn, P. M. Jones, and D. E. Gallardo, "Photochemical Growth of Silver Nanoparticles on c(−) and c(+) Domains on Lead Zirconate Titanate Thin Films," *J. Am. Chem. Soc.*, **129** [28] 8724–8 (2007).

[17]J. A. Basmajian and R. C. DeVries, "Phase Equilibria in the System $BaTiO_3$–$SrTiO_3$," *J Am. Ceram. Soc.*, **40** [11] 373–6 (1957).

[18]W. J. Merz, "Double Hysteresis Loop of $BaTiO_3$ at the Curie Point," *Phys. Rev.*, **91** [3] 513–7 (1953).

[19]A. Ianculescu, L. Mitoseriu, D. Berger, C. E. Ciomaga, D. Piazza, and C. Galassi, "Composition-Dependent Ferroelectric Properties of $Ba_{1-x}Sr_xTiO_3$ Ceramics," *Phase Transitions*, **79** [6 & 7] 375–88 (2006).

[20]M. Cardona, "Optical Properties and Band Structure of $SrTiO_3$ and $BaTiO_3$," *Phys. Rev.*, **140** [2A] A651–5 (1965).

[21]S. H. Wemple, "Polarization Fluctuations and the Optical-Absorption Edge in $BaTiO_3$," *Phys. Rev. B*, **2** [7] 2679–89 (1970).

[22]C. N. Berglund and H. J. Braun, "Optical Absorption in Single-Domain Ferroelectric Barium Titanate," *Phys. Rev.*, **164** [2] 790–9 (1967).

[23]K. W. Blazey, "Optical Absorption Edge of $SrTiO_3$ Around the 105 K Phase Transition," *Phys. Rev. Lett.*, **27** [3] 146–8 (1971).

[24]K.van Benthema, C. Elsässer, and R. H. French, "Bulk Electronic Structure of $SrTiO_3$: Experiment and Theory," *J. Appl. Phys.*, **90** [12] 6156–64 (2001).

[25]L. Hafid, G. Godefroy, A. El Idrissi, and F. Michel-Calendini, "Absorption Spectrum in the Near UV and Electronic Structure of Pure Barium Titanate," *Solid State Comm.*, **66** [8] 841–5 (1988).

[26]H. H. Kung, H. S. Jarrett, A. W. Sleight, and A. Ferretti, "Semiconducting Oxide Anodes in Photoassisted Electrolysis of Water," *J. Appl. Phys.*, **48** [6] 2463–9 (1977).

[27]K. Ohara, T. Ohsawa, H. Koinuma, and Y. Matsumoto, "Photochemical Approach to Analysis of Ferroelectric Transitionin $Ba_xSr_{1-x}TiO_3$ Epitaxial Films," *Jpn. J. Appl. Phys.*, **45** [11] L339–42 (2006).

[28]D. Tiwari, S. Dunn, and Q. Zhang, "Impact of Zr/Ti ratio in the PZT on the photoreduction of silver nanoparticles," *Mater. Res. Bull.*, **44** [6] 1219–24 (2009).

[29]W. J. Albery and P. N. Bartlett, "The Transport and Kinetics of Photogenerated Carriers in Colloidal Semiconductor Electrode Particles," *J. Electrochem. Soc.*, **131** [2] 315–25 (1984).

[30]I. K. Konstantinou and T. A. Albanis, "TiO_2-Assisted Photocatalytic Degradation of Azo Dyes in Aqueous Solution: Kinetic and Mechanistic Investigations—A Review," *Appl. Catal. B Environ.*, **49** [1] 1–14 (2004).

[31]P. S. Rao and A. Hayon, "Reduction of Dyes by Free Radicals in Solution. Correlation Between Reaction Rate Constants and Redox Potentials," *J. Phys. Chem.*, **77** [23] 2753–6 (1973).

[32]L. A. Xue, Y. Chen, and R. J. Brook, "The Influence of Ionic Radii on the Incorporation of Trivalent Dopants into $BaTiO_3$," *Mater. Sci. Eng. B*, **1** [2] 193–201 (1988).

[33]K. Bergmann and C. T. O'Konski, "A Spectroscopic Study of Methylene Blue Monomer, Dimer, and Complexes with Montmorillinite," *J. Phys. Chem.*, **67** [10] 2169–77 (1963).

[34]S. V. Kalinin, C. Y. Johnson, and D. A. Bonnell, "Domain Polarity and Temperature Induced Potential Inversion on the $BaTiO_3$ (100) Surface," *J. Appl. Phys.*, **91** [6] 3816–23 (2002).

[35]A. Bhardwaj, N. V. Burbure, A. Gamalski, and G. S. Rohrer, "Composition Dependence of the Photochemical reduction of Ag by $Ba_{1-x}Sr_xTiO_3$ Solid Solutions," *Chem. Mater.*, **22** [11] 3527–34 (2010).

[36]J. Nowotny and M. Rekas, "Dielectric Ceramics Materials Based on Alkaline Earth Metal Titanates," *Key Eng. Mater.*, **66–67**, 45–144 (1992).

[37]J. P. Remeika, "A Method for Growing Barium Titanate Single Crystals," *J. Am. Chem. Soc.*, **76** [3] 940–1 (1954). □